# What is the dopant concentration in polycrystalline thin-film Cu(In,Ga)Se₂?

F. Werner *, T. Bertram, J. Mengozzi, S. Siebentritt

*Laboratory for Photovoltaics, University of Luxembourg, Rue du Brill 41, L-4422 Belvaux, Luxembourg*

## ARTICLE INFO

## ABSTRACT

We compare the dopant concentration of polycrystalline Cu(In,Ga)Se₂ thin film absorbers derived from Hall and capacitance-voltage measurements. Although both measurements techniques appear to be reliable, dopant concentrations determined by capacitance-voltage analysis are significantly lower and vary with probing depth into the absorber. The doping profiles and differences between both measurement techniques are consistent with Cd in-diffusion from the CdS buffer layer during solar cell fabrication. Different doping profiles obtained after a variation of the CdS deposition process support this scenario.

© 2016 Elsevier B.V. All rights reserved.

## 1. Introduction

The net dopant concentration of the absorber layer is a critical parameter for understanding and optimizing the performance of a thin film solar cell. The dopant concentration for example significantly affects the recombination rate and determines the properties of the space charge region (SCR) at the hetero junction. The two most commonly employed experimental techniques to determine the dopant concentration are electrical measurements of the Hall effect and of the voltage-dependent SCR capacitance ($C$–$V$ measurements). Both are well-established standard characterization techniques and described in a large number of textbooks and review articles (see for example Refs. [1–6] for further information). However, both techniques are often applied to polycrystalline thin film absorbers without sufficient discussion of the validity of the approach, and the dopant concentrations obtained from both measurement techniques for comparable specimens often differ by more than one order of magnitude.

The basic equations governing interpretation of Hall and C–V measurements rely on simplified device models and make several assumptions, which are often not valid in realistic thin film photovoltaic devices. The original proof of the van-der-Pauw technique [7] by conformal mapping is based on the assumption of a homogeneous conductor. Due to the presence of grain boundaries, polycrystalline thin films can no longer be regarded as laterally homogeneous conductors, and care must be taken in the interpretation of Hall measurement on such films. Conventional capacitance-voltage analysis, on the other hand,

assumes a one-sided abrupt $p/n$ junction, relies on an appropriate choice of equivalent electrical circuit, and is susceptible to capacitance contributions by deep defects. Particularly the assumption of a one-sided abrupt $p/n$ junction is difficult to verify independently for typical chalcopyrite solar cells, as the $n$-doped side is formed by a complex multi-layer stack of differently doped buffer and window layers. To further complicate matters, Hall analysis is a lateral technique and requires an insulating substrate, while $C$–$V$ analysis is a perpendicular technique and requires a conductive back contact.

In this contribution we compare Hall and $C$–$V$ measurements of chalcopyrite thin film absorbers and solar cells, and assess the validity of the analysis.

## 2. Experimental details

Polycrystalline Cu(In,Ga)Se₂ (CIGSe) and CuInSe₂ absorbers were grown on blank and Mo-coated soda-lime glass (SLG) by physical vapor deposition in a molecular beam epitaxy system. We determine the chemical composition of the as-grown films by energy-dispersive X-ray (EDX) analysis. The Cu(In,Ga)Se₂ films are slightly Cu-poor with $[Cu]/([Ga] + [In]) \approx 0.98$ and a ratio of $[Ga]/([Ga] + [In]) \approx 0.3$. The CuInSe₂ films are grown under Cu-rich conditions and hence are assumed to be nearly stoichiometric.

We use pairs of blank and Mo-coated SLG substrates in the same deposition run to ensure identical deposition parameters on both types of substrates. The two different types of substrates are necessary because $C$–$V$ analysis requires a conductive back contact, while Hall analysis requires an insulating substrate to prevent parasitic current flow through the back contact. The substrate temperature during growth is controlled

* Corresponding author.
  *E-mail address:* florian.werner@uni.lu (F. Werner).

by an infrared heating source, and thus the additional metallic Mo layer might alter the sample temperature and influence the growth process. In order to exclude any influence of a temperature difference on the dopant concentration, we have mechanically detached the CIGSe film from a Mo-coated glass substrate for Hall measurements. This is achieved by gluing a glass substrate to the top of the CIGSe thin film. Application of mechanical force then leads to a detachment of the CIGSe from the smooth Mo surface.

All samples were etched in KCN after growth to remove any secondary copper-selenide phases and to ensure good electrical contacts. For the fabrication of Hall specimens, triangular gold contacts (contact area below 1 mm$^2$) with a thickness of 300 nm were defined on the corners of 5 × 5 mm$^2$ pieces of the sample by electron beam evaporation through a shadow mask. We determine the majority carrier concentration and Hall mobility by Hall measurements in the van der Pauw configuration [7] under varying magnetic fields of up to 9 T using a superconducting magnet in a closed-cycle cryostat. We assume a Hall scattering factor r of unity and infinitely small contacts. The sample temperature is measured at the back of the sample holder and is calibrated to be correct within ± 1 K. Due to the stabilization time required for the setup, all samples were kept in the dark for at least one day before the measurement.

For C–V analysis, absorbers grown on Mo-coated glass are processed into solar cells by chemical bath deposition of a CdS buffer layer and subsequent rf-sputtering of a double layer of i-ZnO/Al:ZnO. A Ni/Al grid is deposited as front contact by electron beam evaporation through a shadow mask. Individual cells with areas of 0.2–0.5 cm$^2$ are defined by mechanical scribing. After mounting in the shielded and evacuated cryostat, the sample is kept in the dark at a temperature of 300 K for at least one night before the measurement. The impedance spectrum is recorded with an Agilent E4980A Precision LCR Meter at frequencies of 100 Hz–1 MHz and an ac voltage of 30 mV, and the capacitance is extracted assuming a parallel equivalent circuit ("Cp-G" model).

## 3. Results and discussion

### 3.1. Hall analysis

Hall measurements of polycrystalline low-mobility thin films are challenging due to a small signal, limited by a small measurement current, compared to large offset voltages originating from imperfect alignment of the voltage probes on the highly resistive sample [7]. For the measurements in this study we have taken care to correct for these offsets: the sheet resistance is measured at each magnetic field in addition to the Hall voltage to account for resistivity variations, and the Hall coefficient is obtained from the linear slope of the magnetic-field-dependent Hall voltage over a wide range of magnetic fields between −9 T and +9 T. A detailed review of the correction procedures will be published in a separate manuscript. Fig. 1 shows the resulting effective hole concentration p and effective Hall mobility μ obtained by Hall measurements of three different samples as a function of inverse temperature 1000 / T. We compare one absorber grown on glass (black squares), the same device after chemical bath deposition of nominally 50 nm of CdS on top (red circles), and one other absorber grown in the same deposition run on Mo-coated glass and subsequently ripped off (blue triangles). Although we obtain somewhat comparable effective hole concentrations in the range of $3 \times 10^{16}$–$1 \times 10^{17}$ cm$^{-3}$, the effective hole mobility differs by almost two orders of magnitude between the three different samples. For polycrystalline samples, however, the effect of grain boundaries on the Hall analysis has to be taken into account. We employ the model of Jerhot and Snejdar [8], where we assume thermionic emission over a potential barrier for majority carriers. As shown by the lines in Fig. 1 we can reproduce all three sets of data with a single set of material parameters, obtained from a fit to the data in Fig. 1 and summarized in Table 1, which only differ in the barrier height at the grain boundary (in addition, we have to assume a
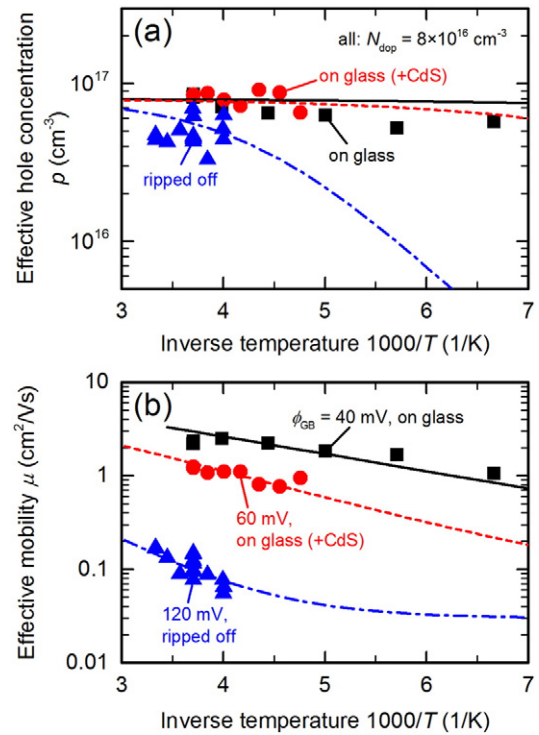


**Fig. 1.** (a) Effective hole concentration and (b) effective mobility obtained by Hall analysis of polycrystalline Cu(In,Ga)Se$_2$ thin film absorbers grown on glass (black squares, solid line), the same sample with nominally 50 nm CdS on top (red circles, dashed line); and grown on Mo-coated glass and then ripped off (blue triangles, dash-dotted line). Lines are best fits to a model of the Hall effect in polycrystalline films. The dopant concentration $N_{dop}$ and barrier height at the grain boundary $\phi_{GB}$ are given in the graph, all parameters are summarized in Table 1.

slightly lower mobility within the grain boundaries after rip-off, which might be related to mechanical damage or glue entering the grain boundaries). The excellent agreement between model and experiment strongly supports the validity of the analysis and allows to derive the real in-grain carrier concentration from the measured apparent hole concentration. This leads to the conclusion that Hall analysis on polycrystalline CIGSe yields consistent and reliable results if grain boundaries are taken into account. Furthermore, the presence of a Mo back contact during the growth process does not significantly affect the dopant concentration in the absorber film, neither does ripping off the film modify the in-grain "bulk". The dopant concentration of all three films shown in Fig. 1, obtained by Hall analysis, is then $(8 \pm 3) \times 10^{16}$ cm$^{-3}$.

### 3.2. Capacitance–voltage analysis

For a direct comparison, we process solar cells from absorbers grown on Mo-coated glass in the same deposition run as those analyzed by Hall analysis in Section 3.1. Fig. 2(a) shows the inverse squared capacitance

**Table 1**
Model parameters for the Hall analysis taking into account the effect of grain boundaries (GB), obtained by fitting the temperature-dependent Hall data.

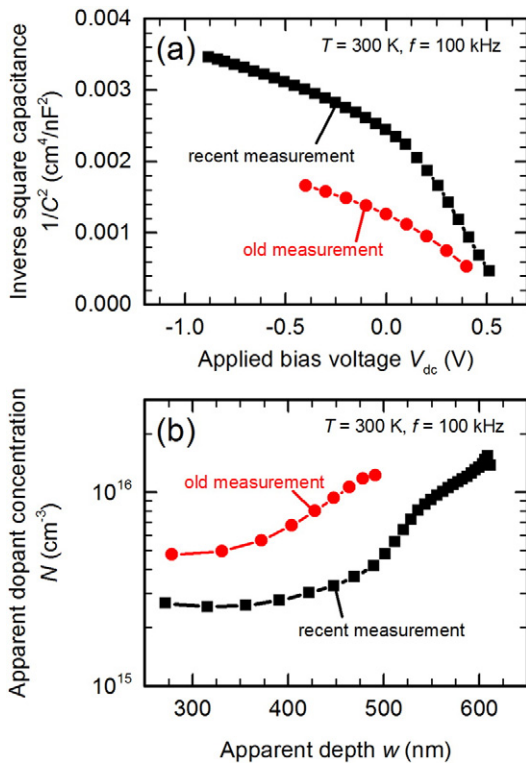| Model parameter | Value |
|---|---|
| Dopant concentration | $8 \times 10^{16}$ cm$^{-3}$ |
| GB barrier height | 40/60/120 mV |
| In-grain mobility | 30 cm$^2$/Vs |
| GB mobility | 0.9 cm$^2$/Vs |
| - after rip-off | 0.6 cm$^2$/Vs |
| Relative size GB/grain | 0.05 |

**Fig. 2.** (a) Inverse square capacitance $1/C^2$ as a function of applied bias voltage $V_{dc}$ and (b) apparent dopant concentration $N$ as a function of apparent depth $w$ of a Cu(In,Ga)Se$_2$ absorber grown on Mo-coated glass. The sample has been stored for 15 months in vacuum between both measurements.

$1/C^2$ as a function of applied bias voltage $V_{dc}$, the so-called "Mott-Schottky" plot, at a sample temperature of $T = 300$ K and an ac frequency of $f = 100$ kHz. Shown are measurements of the same sample 2 months after fabrication of the solar cell (red circles), and a recent measurement 15 months later (black squares). Between both measurements, the samples have been stored in vacuum without special shielding against ambient light. For an ideal one-sided junction in a homogeneously doped semiconductor, the Mott-Schottky plot is expected to yield a straight line with a slope inversely proportional to the semiconductor dopant concentration [2,4–6]. This is obviously not the case for our measurements, and the extracted dopant concentration will depend on the bias range chosen for the analysis. Such behavior is well known and commonly attributed to one of two alternative explanations:

- **Dopant gradient:** The ac test voltage applied during a $C$–$V$ measurement causes a slight widening and shrinking of the space charge region in each measurement cycle, and a $C$–$V$ measurement hence probes the dopant concentration at the edge of the space charge region (commonly denoted as "apparent depth"). The width of the space charge region changes with applied dc bias, as shown in the sketch in Fig. 3, and any depth-dependence of the dopant concentration would thus be observed as a change of the slope of the Mott-Schottky plot.
- **Deep defects:** In reverse bias, the applied bias voltage causes a strong *downward* band bending in the space charge region, and accordingly the valence band edge moves further from the majority carrier Fermi level $E_F$. For sufficient reverse bias, the Fermi level will thus cross the energetic level of a deep defect at some depth within the space charge region, as sketched in Fig. 3(a). A change in bias voltage will then charge or discharge defects near the Fermi level, and this additional charge will appear as an additional apparent dopant concentration in the $C$–$V$ analysis. For sufficiently high forward bias, the defect level is above the Fermi level everywhere in the device, as shown in Fig. 3(b). The charge state of the defect thus does not change and does not influence the measurement.

In the case of deep defects, the true bulk dopant concentration would be obtained from the slope of the Mott-Schottky plot in forward bias. For the CIGSe device shown in Fig. 2, assuming a relative dielectric permittivity of $\varepsilon_r = 13.6$ [9], this would yield a dopant concentration of $(2$–$6) \times 10^{15}$ cm$^{-3}$, which is at least one order of magnitude lower than the value of $(8 \pm 3) \times 10^{16}$ cm$^{-3}$ obtained by Hall analysis in Section 3.1.

Such a striking disagreement might be related to the complex structure of the different layers in a thin film solar cell. Care must be taken to ensure that the measured capacitance is indeed indicative of the space charge capacitance of the main junction. Additional elements of the electrical equivalent circuit, e.g., parasitic resistances and diode conductance, can be identified and corrected for by analyzing the frequency-dependent impedance spectrum (not shown here). These additional circuit elements have a negligible impact on the extracted dopant concentration in reverse and low forward bias for reasonable values of shunt and series resistance, but might cause an apparent increase of the dopant concentration in higher forward bias (small apparent depth) as a measurement artifact. Note also, that the actual dc bias
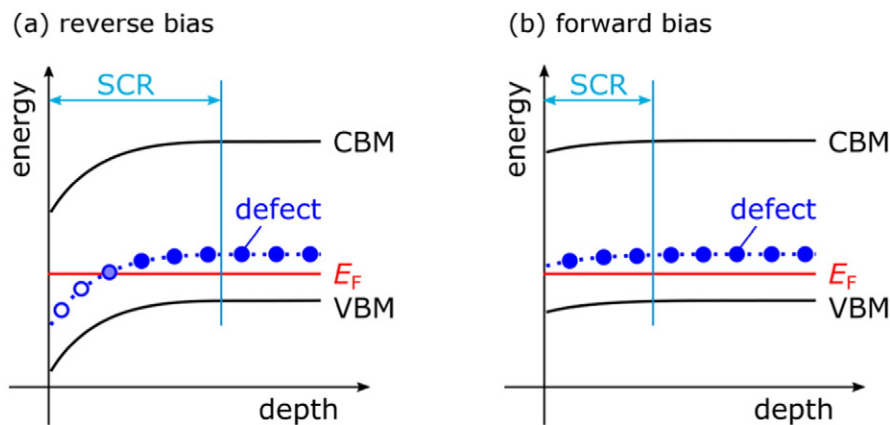


**Fig. 3.** Qualitative sketch of the band diagram in the CIGSe absorber for (a) reverse and (b) forward bias. Shown are the valence band maximum (VBM), conduction band minimum (CBM), majority carrier Fermi level $E_F$, and a defect level (blue symbols and lines) as a function of depth below the CIGSe/CdS interface. The extension of the space charge region (SCR) is indicated with a blue arrow.

voltage applied across the device will deviate significantly from the set value, unless the total impedance of the solar cells is far higher than the output impedance of the LCR meter ($\approx 100\ \Omega$ for the Agilent E4980A).

An erroneously low capacitance, and thus dopant concentration, might however be related to a second capacitance in series with the SCR capacitance within the CIGSe, which would reduce the measured total device capacitance. The classical model of a one-sided step-junction assumes a highly doped ZnO window and either a highly-doped or depleted CdS buffer layer. The capacitance contributions from these layers then are either negligible (highly-doped CdS), or only influence the build-in potential and SCR width, without affecting the dopant concentration extracted from the slope of $C^{-2}$ vs. $V$ (depleted CdS) [6]. Most notably, the high absorber doping obtained by Hall analysis requires an even higher net dopant concentration ($n \gg 10^{17}\ \mathrm{cm}^{-3}$) in the CdS buffer and ZnO window to still ensure a one-sided $p/n$-junction, which might not be fulfilled in a realistic device. We have run one-dimensional device simulations using the program SCAPS [10] to test whether the presence of buffer and window layers could cause apparent dopant profiles as shown in Fig. 2(b) despite a constant absorber doping of $8 \times 10^{16}\ \mathrm{cm}^{-3}$, as obtained by Hall analysis. We simulate the capacitance–voltage relation $C(V)$ for ZnO and CdS dopant concentrations between $10^{15}\ \mathrm{cm}^{-3}$ and $10^{19}\ \mathrm{cm}^{-3}$, and conduction band offsets at the CIGSe/CdS interface of up to $+0.5$ eV. Although the shapes of the dopant profiles extracted from the slope of the simulated $C^{-2}$ vs. $V$ curves are qualitatively similar to those observed experimentally, the simulated apparent dopant concentrations differ from the constant absorber doping defined in the simulation by only a factor of up to 2 for low buffer or window dopant concentrations or high conduction band offsets. Similar results with a comparable deviation of dopant concentrations by a factor of 2 have recently been presented by Sozzi et al. [11]. Although low buffer or window doping or a high conduction band offset indeed influences the apparent dopant concentration extracted from a $C$–$V$ measurement, the difference is much smaller than observed experimentally. In particular, these effects cannot fully explain the difference of one order of magnitude between $C$–$V$ and Hall analysis.

We find that the "U"-shape of the apparent dopant concentration for CIGSe as shown in Fig. 2(b) at the moment cannot be explained quantitatively by either deep defects or parasitic circuit elements, particularly buffer and window layers. We therefore propose that it in fact originates at least partly from an actual variation of dopant concentration with depth into the CIGSe bulk. The most likely origin of this depth-dependence is cadmium in-diffusion from the CdS buffer layer into the CIGSe absorber. Theoretical calculations show that Cd acts as a donor in CIGSe [12–14], which would thus lead to an increased compensation ratio near the CIGSe/CdS interface and accordingly reduce the net doping in the space charge region. Several studies provide direct evidence for Cd in-diffusion into CIGSe, at least within a few tens of nanometers from the CdS/CIGSe interface [15–19]. Note however, that parts-per-million concentrations of electrically active Cd are sufficient to significantly affect the net doping, which is well below typical detection limits. The different dopant profiles observed in Fig. 2 for the same sample some time apart can then be interpreted as additional Cd in-diffusion over time. The initial Cd in-diffusion might occur rapidly, which could explain why even the initial measurement after sample fabrication (red circles in Fig. 2) already shows a significantly reduced dopant concentration compared to the Hall measurement. The red circles shown in Fig. 1 indicate that no significant change of the dopant concentration is observed if nominally 50 nm of CdS are deposited onto the CIGSe Hall specimen. This requires further investigations, but it appears reasonable that any variation of surface-near dopant concentration only has a diminished influence on the Hall analysis, which probes current flow throughout the full thickness of the CIGSe absorber layer of roughly 2.5 μm. Furthermore, sputter deposition of the ZnO window layer might also affect the Cd diffusion.
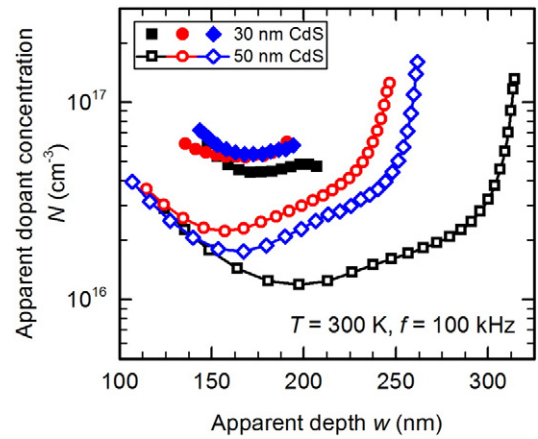


**Fig. 4.** Apparent dopant concentration $N$ as a function of apparent depth $w$ of three different CuInSe$_2$ grown with different Se supply. Different cells with nominally 30 nm CdS (solid symbols) and 50 nm CdS (open symbols) buffer layers were measured for each absorber.

In order to obtain further evidence of the impact of Cd on the dopant concentration we processed several polycrystalline CuInSe$_2$ absorbers into solar cells with different thicknesses of the CdS buffer layer. We selected three different absorbers grown with different Se supply, which result in slightly different bulk dopant and defect concentrations. Most notably, the copper-to-indium atomic ratios determined by EDX, before etching a Cu$_x$Se secondary phase, are [Cu]:[In] = 1.18 (black squares in Fig. 4), 1.22 (blue diamonds), and 1.30 (red circles), respectively [20]. For one batch of samples, the chemical bath deposition of the CdS buffer layer was reduced to 60% of the standard duration, corresponding to a nominal thickness of the CdS layer of 30 nm. A second batch of samples was processes with the standard recipe, corresponding to nominally 50 nm of CdS. Fig. 4 shows the apparent dopant concentration as a function of apparent depth (space charge region width) obtained by $C$–$V$ analysis for the thin (closed symbols) and thick (open symbols) CdS buffer layers. All samples with thin CdS buffer show a significantly higher dopant concentration compared to the standard 50 nm CdS buffer layer, presumably due to a reduced Cd in-diffusion limited by the smaller reservoir of Cd atoms in the thin CdS buffer. All samples with the standard 50 nm CdS buffer show the typical depth-dependence of the dopant concentration already observed in Fig. 2 for CIGSe. For these samples, the dopant concentration exceeds $10^{17}\ \mathrm{cm}^{-3}$ deeper into the CuInSe$_2$ bulk, about one order of magnitude higher than the minimum dopant concentration of $(1$–$2) \times 10^{16}\ \mathrm{cm}^{-3}$ extracted in weak forward bias. The observed trend of reduced surface-near net doping for samples with lower [Cu]:[In] ratio supports earlier observations, which relate Cd diffusion in CuInSe$_2$ to copper vacancies [13–19]. Note that the increase in dopant concentration towards *smaller* apparent depth, i.e., in stronger forward bias, most likely is a measurement artifact due to additional equivalent circuit elements as mentioned above.

## 4. Conclusions

The dopant concentration of a set of polycrystalline Cu(In,Ga)Se$_2$ thin film absorbers from the same deposition run was measured by Hall and capacitance-voltage analysis. Taking into account the influence of grain boundaries on the Hall analysis, the dopant concentration derived by Hall analysis was shown to be $(8 \pm 3) \times 10^{16}\ \mathrm{cm}^{-3}$. This dopant concentration is the same for absorbers grown directly on glass and for absorbers grown on Mo-coated glass and then mechanically ripped off for Hall measurements. In contrast, the dopant concentration obtained by capacitance-voltage analysis of solar cells fabricated from the same absorbers was shown to be depth-dependent and significantly lower than the value obtained by Hall analysis. This discrepancy between Hall and capacitance-voltage analysis is a clear indication that the

commonly used simplified interpretation of capacitance-voltage data must be modified for CIGSe thin film solar cells. Measurement artifacts due to deep defects or buffer/window layers were shown to be insufficient to explain this discrepancy. The depth-dependent doping profile was shown to depend critically on the thickness of the CdS buffer layer in solar cells fabricated from different CuInSe$_2$ absorbers. We propose that the differences between Hall and capacitance-voltage analysis, as well as the depth-dependent doping profile measured on solar cells, might be related to Cd in-diffusion from the CdS buffer layer into the absorber film, where Cd increases the surface-near donor concentration and thus reduces the net doping. Accordingly, a depth-dependent dopant concentration is an additional effect to be considered in addition to deep defects and parasitic circuit elements in the interpretation of capacitance-voltage measurements.

## References

[1] E.H. Putley, The Hall Effect and Related Phenomena, Butterworths, London, UK, 1960.
[2] P. Blood, J.W. Orton, The Electrical Characterization of Semiconductors: Majority Carriers and Electron States, Academic Press, London, UK, 1992.
[3] A. Beer, The Hall effect and related phenomena, Solid State Electron. 9 (1966) 339–351.
[4] D.K. Schroder, Semiconductor Material and Device Characterization, John Wiley & Sons, New York, 1990 41–45.
[5] S.M. Sze, Physics of Semiconductor Devices, second ed John Wiley & Sons, New York, 1981 74–84.
[6] R. Scheer, H.-W. Schock, Chalcogenide Photovoltaics, Wiley-VCH Verlag, Weinheim, Germany, 2011 119–122.
[7] L.J. van der Pauw, A method of measuring the resistivity and Hall coefficient on lamellae of arbitrary shape, Philips Tech. Rev. 20 (1958) 220–224.
[8] J. Jerhot, V. Snejdar, Hall effect in polycrystalline semiconductors, Thin Solid Films 52 (1978) 379.
[9] P. Li, R. Anderson, R. Plovnick, Dielectric constant of CuInSe$_2$ by capacitance measurements, J. Phys. Chem. Solids 40 (1979) 333–334.
[10] M. Burgelman, P. Nollet, S. Degrave, Modelling polycrystalline semiconductor solar cells, Thin Solid Films 361–362 (2000) 527–532.
[11] G. Sozzi, M. Lazzarini, R. Menozzi, R. Carron, E. Avancini, B. Bissig, S. Buecheler, A.N. Tiwari, A numerical study of the use of C-V characteristics to extract the doping density of CIGS absorbers, Proc. 43rd IEEE-PVSC, Portland, OR, 2016.
[12] C. Persson, S. Lany, Y.-J. Zhao, A. Zunger, n-Type doping of CuInSe$_2$ and CuGaSe$_2$, Phys. Rev. B 72 (2005) 035211.
[13] T. Maeda, T. Wada, First-principles studies on Cd doping in CuInSe$_2$ and related compounds during chemical bath deposition of CdS buffer layer, Jpn. J. Appl. Phys. 52 (2013) 061201.
[14] J.B. Varley, V. Lordi, Intermixing at the absorber-buffer layer interface in thin-film solar cells: the electronic effects of point defects in Cu(In,Ga)(Se,S)$_2$ and Cu$_2$ZnSn(Se,S)$_4$ devices, J. Appl. Phys. 116 (2014) 063505.
[15] D. Liao, A. Rockett, Cd doping at the CuInSe$_2$/CdS heterojunction, J. Appl. Phys. 93 (2003) 9380–9382.
[16] K. Ramanathan, R. Noufi, J. Granata, J. Webb, J. Keane, Prospects for in situ junction formation in CuInSe$_2$ based solar cells, Sol. Energ. Mat. Sol. 55 (1998) 15–22.
[17] T. Nakada, A. Kunioka, Direct evidence of Cd diffusion into Cu(In,Ga)Se$_2$ thin films during chemical-bath deposition process of CdS films, Appl. Phys. Lett. 74 (1999) 2444–2446.
[18] D. Abou-Ras, G. Kostorz, A. Romeo, D. Rudmann, A. Tiwari, Structural and chemical investigations of CBD- and PVD-CdS buffer layers and interfaces in Cu(In,Ga)Se$_2$-based thin film solar cells, Thin Solid Films 480-481 (2005) 118–123.
[19] B. Ümsür, W. Calvet, B. Höpfner, A. Steigert, I. Lauermann, M. Gorgoi, K. Prietzel, H. Navirian, C. Kaufmann, T. Unold, M.C. Lux-Steiner, Investigation of Cu-poor and Cu-rich Cu(In,Ga)Se$_2$/CdS interfaces using hard X-ray photoelectron spectroscopy, Thin Solid Films 582 (2015) 366–370.
[20] V. Deprédurand, T. Bertram, S. Siebentritt, Influence of the Se environment on Cu-rich CIS devices, Physica B 439 (2014) 101–104.